DESY 00-026
UdeM-GPP-TH-00-68
hep-ph/0002167
February 2000

arXiv:hep-ph/0002167 v2 22 Feb 2000

CP VIOLATION AND QUARK MIXING

Ahmed Ali
Deutsches Elektronen Synchrotron DESY, Hamburg
Notkestrae 85, D-22603 Hamburg

David London
Laboratoire René J.-A. Lévesque, Université de Montréal,
Montréal, QC, Canada H3C 3J7

Invited Talk. To be published in the Proceedings of the 3rd Workshop on Physics and Detectors for DAΦNE, Frascati, Italy, Nov. 16 – 19, 1999

Frascati Physics Series Vol. XVI (2000),
PHYSICS AND DETECTORS FOR DAΦNE – Frascati, Nov. 16-19, 1999

CP VIOLATION AND QUARK MIXING

Ahmed Ali
Deutsches Elektronen Synchrotron DESY, Hamburg

David London
Laboratoire René J.-A. Lévesque, Université de Montréal,
Montréal, QC, Canada H3C 3J7

ABSTRACT

Measurements of CP asymmetries in B decays will soon be made at B factories and hadron machines. In light of this, we review and update the profile of the CKM unitarity triangle and the resulting CP asymmetries in B decays. This is done both in the standard model and in several variants of the minimal supersymmetric standard model (MSSM), which are characterized by a single phase in the quark flavour mixing matrix. After imposing present constraints on the parameters of these models, the predicted ranges of $\sin 2\beta$ in the standard model and in the MSSM are found to be similar. However, these theories may be distinguished by future precise measurements of the other two CP-violating phases α and γ.

1 Introduction

Within the standard model (SM), CP violation is due to the presence of a nonzero complex phase in the Cabibbo-Kobayashi-Maskawa (CKM) quark mixing matrix V [1]. A particularly useful parametrization of the CKM matrix, due to Wolfenstein [2], follows from the observation that the elements of this matrix exhibit a hierarchy in terms of λ, the Cabibbo angle. In this parametrization the CKM matrix can be written approximately as

$$V \simeq \begin{pmatrix} 1-\frac{1}{2}\lambda^2 & \lambda & A\lambda^3\,(\rho-i\eta) \\ -\lambda(1+iA^2\lambda^4\eta) & 1-\frac{1}{2}\lambda^2 & A\lambda^2 \\ A\lambda^3\,(1-\rho-i\eta) & -A\lambda^2 & 1 \end{pmatrix} \ . \tag{1}$$

The allowed region in ρ–η space can be elegantly displayed using the so-called unitarity triangle (UT). The unitarity of the CKM matrix leads to the following relation:

$$V_{ud}V_{ub}^* + V_{cd}V_{cb}^* + V_{td}V_{tb}^* = 0 \ . \tag{2}$$

Using the form of the CKM matrix in Eq. (1), this can be recast as

$$\frac{V_{ub}^*}{\lambda V_{cb}} + \frac{V_{td}}{\lambda V_{cb}} = 1 \ , \tag{3}$$

which is a triangle relation in the complex plane (i.e. ρ–η space). With the experimental precision expected in future B (and K) decays, it may become necessary to go beyond leading order in λ in the Wolfenstein parametrization given above. To this end, we follow here the prescription of Buras et al. [3]: defining $\bar\rho \equiv \rho(1-\lambda^2/2)$ and $\bar\eta \equiv \eta(1-\lambda^2/2)$, we have

$$V_{us} = \lambda, \quad V_{cb} = A\lambda^2, \quad V_{ub} = A\lambda^3(\rho - i\eta), \quad V_{td} = A\lambda^3(1-\bar\rho - i\bar\eta) \tag{4}$$

The key point here is that the matrix elements V_{us}, V_{cb} and V_{ub} remain unchanged, but V_{td} is renormalized in going from leading order (LO) to next-to-leading order (NLO). The apex of the UT is now defined by $(\bar\rho, \bar\eta)$.

Constraints on $\bar\rho$ and $\bar\eta$ come from a variety of sources. For example, $|V_{cb}|$ and $|V_{ub}|$ can be extracted from semileptonic B decays, and $|V_{td}|$ is at present probed in B_d^0–$\overline{B_d^0}$ mixing. The interior CP-violating angles α, β and γ can be measured through CP asymmetries in B decays. Additional constraints come from CP violation in the kaon system ($|\epsilon|$), as well as B_s^0–$\overline{B_s^0}$ mixing.

A profile of the unitarity triangle was presented by us in early 1999 [4]. This analysis was done at NLO precision, taking into account the state-of-the-art calculations of the hadronic matrix elements from lattice QCD and data available at that time. Subsequently, an improved lower limit $\Delta M_s > 14.3\ (\mathrm{ps})^{-1}$ was reported at the Lepton-Photon symposium in the summer of 1999 [5]. In this report, we update the results of our 1999 CKM-unitarity fits by incorporating this new limit on ΔM_s. As we shall see here, this measurement tightens the constraints on the CKM parameters. The other new ingredient in our fits is that we now use the improved Wolfenstein parametrization given in Eq. (4). We also compare our results with two other recent fits in which the new ΔM_s-limit has been incorporated [6, 7], but which differ from us in details which we shall specify below.

If new physics (of any type) is present, the principal way in which it can enter in flavour physics is via new contributions, possibly with new phases, to K^0–$\overline{K^0}$, B^0_d–$\overline{B^0_d}$ and B^0_s–$\overline{B^0_s}$ mixing. The tree decay amplitudes, being dominated by virtual W exchange, remain essentially unaffected by new physics. Thus, even in the presence of new physics, the measured values of $|V_{cb}|$ and $|V_{ub}|$ correspond to their true SM values, so that two sides of the UT are unaffected. However, the third side, which depends on $|V_{td}|$, will in general be affected by new physics. Furthermore, the measurements of $|\epsilon|$ and B^0_s–$\overline{B^0_s}$ mixing, which provide additional constraints on the UT, will also be affected. If Nature is kind, the unitarity triangle, as constructed from direct measurements of α, β and γ, will be inconsistent with that obtained from independent measurements of the sides. If this were to happen, it would be clear evidence for the presence of physics beyond the SM, and would be most exciting. In such a case, the new physics is also expected to modify the decay rates and distributions of rare B-decays such as $B \to X_s\gamma$, $B \to X_s\ell^+\ell^-$ and $B \to X_s\nu\bar{\nu}$, and of related exclusive decays. (Similarly, the corresponding decays dominated by the $b \to d$ transitions may also be affected.)

One type of new physics which has been extensively studied is supersymmetry (SUSY). A hint suggesting that SUSY might indeed be around the corner is the gauge-coupling unification: a supersymmetric grand unified theory does better than its non-supersymmetric counterpart. A great deal of effort has gone into a systematic study of the pattern of flavour violation in SUSY, in particular in the flavour-changing neutral-current processes in K and

B decays. We shall concentrate here on the minimal supersymmetric standard model (MSSM), and update the anticipated profile of the UT and CP-phases which we presented earlier [4]. Of particular interest here is the scenario of minimal supersymmetric flavour violation [8], which involves, in addition to the SM degrees of freedom, charged Higgs bosons, a light stop (assumed right-handed) and a light chargino, with all other degrees of freedom assumed heavy and hence effectively integrated out. This scenario can be embedded in supergravity (SUGRA) models with gauge-mediated supersymmetry breaking, in which the first two squark generations and the gluinos are assumed heavy. Regardless of which variant is used, the key assumption in our analysis is that there are no new phases in the couplings – although there are many new contributions to meson mixing and rare decays, all are proportional to the same combination of CKM matrix elements as found in the SM. As explained above, in this class of models measurements of the CP phases will yield the true SM values for these quantities. However, measurements of meson mixing and rare decays will be affected by the presence of this new physics.

In Section 2, we discuss the profile of the unitarity triangle within the SM. We describe the input data used in the fits and present the allowed region in ρ–η space, as well as the presently-allowed ranges for the CP angles α, β and γ. We turn to supersymmetric models in Section 3. We review several variants of the MSSM, in which the new CP-violating phases are essentially zero. We also discuss the NLO corrections in such models and show that the SUSY contributions to K^0–$\overline{K^0}$, B_d^0–$\overline{B_d^0}$ and B_s^0–$\overline{B_s^0}$ mixing are of the same form and can be characterized by a single parameter f. We compare the profile of the unitarity triangle in SUSY models, for various values of f, with that of the SM. We conclude in Section 4.

2 Unitarity Triangle: SM Profile

2.1 Input Data

We briefly describe below the experimental and theoretical data which constrain the CKM parameters. (For more details, we refer the reader to [4].) A summary can be found in Table 1.

- The CKM parameters λ, A, ρ and η are directly constrained through measurements of the CKM elements $|V_{us}| = \lambda$ [9], $|V_{cb}|$ [9] and $|V_{ub}/V_{cb}|$ [10].

In our fits we ignore the small error on λ. Also, the error on $|V_{ub}/V_{cb}|$ includes some theoretical model dependence.

- $|\epsilon|, \hat{B}_K$: In the standard model, $|\epsilon|$ is essentially proportional to the imaginary part of the box diagram for K^0–$\overline{K^0}$ mixing and is given by [11]

$$|\epsilon| = \frac{G_F^2 f_K^2 M_K M_W^2}{6\sqrt{2}\pi^2 \Delta M_K} \hat{B}_K \left(A^2\lambda^6\bar{\eta}\right) \left(y_c \left\{\hat{\eta}_{ct} f_3(y_c, y_t) - \hat{\eta}_{cc}\right\} + \hat{\eta}_{tt} y_t f_2(y_t) A^2\lambda^4(1-\bar{\rho})\right), \quad (5)$$

where $y_i \equiv m_i^2/M_W^2$, and the functions f_2 and f_3 can be seen in [12]. Here, the $\hat{\eta}_i$ are QCD correction factors, calculated at next-to-leading order in Refs. [13] ($\hat{\eta}_{cc}$), [14] ($\hat{\eta}_{tt}$) and [15] ($\hat{\eta}_{ct}$). The theoretical hadronic uncertainty in the expression for $|\epsilon|$ is in the renormalization-scale independent parameter $\hat{B}_K$. In Table 1, the $|\epsilon|$ entry is taken from Ref. [9], while that for $\hat{B}_K$ is based on lattice QCD methods, summarized in Ref. [16].

- $\Delta M_d, f_{B_d}^2 \hat{B}_{B_d}$: The mass difference ΔM_d is calculated from the B_d^0–$\overline{B_d^0}$ box diagram, which is dominated by t-quark exchange:

$$\Delta M_d = \frac{G_F^2}{6\pi^2} M_W^2 M_B \left(f_{B_d}^2 \hat{B}_{B_d}\right) \hat{\eta}_B y_t f_2(y_t) |V_{td}^* V_{tb}|^2 \ , \quad (6)$$

where, using Eq. (1), $|V_{td}^* V_{tb}|^2 = A^2\lambda^6[(1-\bar{\rho})^2 + \bar{\eta}^2]$. Here, $\hat{\eta}_B = 0.55$ is the QCD correction, calculated in the $\overline{MS}$ scheme [14]. Consistency requires that the top quark mass be rescaled from its pole (mass) value of $m_t = 175 \pm 5$ GeV to the value $\overline{m_t}(m_t(pole)) = 165 \pm 5$ GeV in the $\overline{MS}$ scheme. The slight dependence of $\hat{\eta}_B$ on $\overline{m_t}(m_t(pole))$ in the range given here is ignored. The entry for ΔM_d in Table 1 is taken from Ref. [5].

For the B system, the hadronic uncertainty is given by $f_{B_d}^2 \hat{B}_{B_d}$, analogous to $\hat{B}_K$ in the kaon system. Present estimates of this quantity are summarized in Ref. [16], yielding $f_{B_d}\sqrt{\hat{B}_{B_d}} = (190 \pm 23)$ MeV in the quenched approximation. The effect of unquenching is not yet understood completely. Taking the MILC collaboration estimates of unquenching would increase the central value of $f_{B_d}\sqrt{\hat{B}_{B_d}}$ by 21 MeV [17]. The range of $f_{B_d}\sqrt{\hat{B}_{B_d}}$ given in Table 1 is chosen to take all these considerations into account.

- ΔM_s, $f_{B_s}^2 \hat{B}_{B_s}$: Mixing in the B_s^0–$\overline{B_s^0}$ system is quite similar to that in the B_d^0–$\overline{B_d^0}$ system. The B_s^0–$\overline{B_s^0}$ box diagram is again dominated by t-quark exchange, and the mass difference between the mass eigenstates ΔM_s is given by a formula analogous to that of Eq. (6):

$$\Delta M_s = \frac{G_F^2}{6\pi^2} M_W^2 M_{B_s} \left(f_{B_s}^2 \hat{B}_{B_s} \right) \hat{\eta}_{B_s} y_t f_2(y_t) |V_{ts}^* V_{tb}|^2 \ . \tag{7}$$

Using the fact that $|V_{cb}| = |V_{ts}|$ (Eq. (1)), it is clear that one of the sides of the unitarity triangle, $|V_{td}/\lambda V_{cb}|$, can be obtained from the ratio of ΔM_d and ΔM_s,

$$\frac{\Delta M_s}{\Delta M_d} = \frac{\hat{\eta}_{B_s} M_{B_s} \left(f_{B_s}^2 \hat{B}_{B_s} \right)}{\hat{\eta}_{B_d} M_{B_d} \left(f_{B_d}^2 \hat{B}_{B_d} \right)} \left| \frac{V_{ts}}{V_{td}} \right|^2 \ . \tag{8}$$

The only real uncertainty in this quantity is the ratio of hadronic matrix elements $f_{B_s}^2 \hat{B}_{B_s} / f_{B_d}^2 \hat{B}_{B_d}$. It is now widely accepted that the ratio $\xi_s \equiv (f_{B_s}\sqrt{\hat{B}_{B_s}})/(f_{B_d}\sqrt{\hat{B}_{B_d}})$ is probably the most reliable of the lattice-QCD estimates in B physics. The value given Table 1 is based on Ref. [16].

The present lower bound on ΔM_s is: $\Delta M_s > 14.3\ (\mathrm{ps})^{-1}$ (at 95% C.L.) [5]. This bound has been established using the so-called "amplitude method" [18], and we follow this method in including the current information about B_s^0–$\overline{B_s^0}$ mixing in the fits.

Referring to Table 1, we see that the quantities with the largest errors are $\hat{\eta}_{cc}$ (28%), $\hat{B}_K$ (16%), $|V_{ub}/V_{cb}|$ (15%) and $f_{B_d}\sqrt{\hat{B}_{B_d}}$ (19%). Of these, the latter three are extremely important in defining the allowed ρ–η region (the large error on $\hat{\eta}_{cc}$ does not affect the fit very much). The errors on two of these quantities — $\hat{B}_K$ and $f_{B_d}\sqrt{\hat{B}_{B_d}}$ — are purely theoretical in origin, and the error on $|V_{ub}/V_{cb}|$ has a significant theoretical component (model dependence). Thus, the present uncertainty in the shape of the unitarity triangle is due in large part to theoretical errors. Reducing these errors will be quite important in getting a precise profile of the unitarity triangle and the CP-violating phases.

There are two other measurements which should be mentioned here. First, the KTEV collaboration [19] at Fermilab and the NA48 collaboration [20] at

Table 1: *Data used in the CKM fits*

Parameter	Value
λ	0.2196
$\|V_{cb}\|$	0.0395 ± 0.0017
$\|V_{ub}/V_{cb}\|$	0.093 ± 0.014
$\|\epsilon\|$	$(2.280 \pm 0.013) \times 10^{-3}$
ΔM_d	$(0.473 \pm 0.016)\ (ps)^{-1}$
ΔM_s	$> 14.3\ (ps)^{-1}$
$\overline{m_t}(m_t(pole))$	(165 ± 5) GeV
$\overline{m_c}(m_c(pole))$	1.25 ± 0.05 GeV
$\hat{\eta}_B$	0.55
$\hat{\eta}_{cc}$	1.38 ± 0.53
$\hat{\eta}_{ct}$	0.47 ± 0.04
$\hat{\eta}_{tt}$	0.57
$\hat{B}_K$	0.94 ± 0.15
$f_{B_d}\sqrt{\hat{B}_{B_d}}$	215 ± 40 MeV
ξ_s	1.14 ± 0.06

CERN have reported in 1999 new measurements of direct CP violation in the K sector through the ratio ϵ'/ϵ. Their results, together with those of the earlier experiments NA31 [21] and E731 [22] are as follows:

$$\begin{aligned} \mathrm{Re}(\epsilon'/\epsilon) &= (28.0 \pm 4.1) \times 10^{-4} \quad \text{[KTEV '99]}, \\ &= (18.5 \pm 7.3) \times 10^{-4} \quad \text{[NA48 '99]}, \\ &= (23.0 \pm 6.5) \times 10^{-4} \quad \text{[NA31 '93]}, \\ &= (7.4 \pm 5.9) \times 10^{-4} \quad \text{[E731 '93]}, \end{aligned} \tag{9}$$

yielding the present world average [7] $\mathrm{Re}(\epsilon'/\epsilon) = (21.2 \pm 4.6) \times 10^{-4}$. This combined result excludes the superweak model [23].

A great deal of theoretical effort has gone into calculating this quantity at next-to-leading order accuracy in the SM [24]. However, numerical estimates require a number of non-perturbative parameters, which are at present poorly known [25], yielding an theoretical uncertainty which is larger than an order of magnitude. Thus, whereas ϵ'/ϵ represents a landmark measurement, removing the superweak model of Wolfenstein from further consideration, its impact on CKM phenomenology, particularly in constraining the CKM parameters, is

marginal as ϵ'/ϵ is dominated by non-perturbative uncertainties.

Second, the CDF collaboration has recently made a measurement of $\sin 2\beta$ [26]. In the Wolfenstein parametrization, $-\beta$ is the phase of the CKM matrix element V_{td}. From Eq. (1) one can readily find that

$$\sin(2\beta) = \frac{2\bar{\eta}(1-\bar{\rho})}{(1-\bar{\rho})^2 + \bar{\eta}^2} \ . \tag{10}$$

Thus, a measurement of $\sin 2\beta$ would put a strong contraint on the parameters $\bar{\rho}$ and $\bar{\eta}$. However, the CDF measurement gives [26]

$$\sin 2\beta = 0.79^{+0.41}_{-0.44} \ , \tag{11}$$

or $\sin 2\beta > 0$ at 93% C.L. As we will see in the next section, this constraint is quite weak – the indirect measurement (reported here) already constrains $0.53 \leq \sin 2\beta \leq 0.93$ at the 95% C.L. in the SM. In view of this, and given that it is not clear how to combine the above measurement (which allows for unphysical values of $\sin 2\beta$) with the other data, we have not included this measurement in our fits.

2.2 SM Fits

In order to find the allowed region in $\bar{\rho}$–$\bar{\eta}$ space, i.e. the allowed shapes of the unitarity triangle, the computer program MINUIT is used to fit the parameters to the constraints described above. In the fit, we allow ten parameters to vary: $\bar{\rho}$, $\bar{\eta}$, A, m_t, m_c, η_{cc}, η_{ct}, $f_{B_d}\sqrt{\hat{B}_{B_d}}$, $\hat{B}_K$, and ξ_s. The ΔM_s constraint is included using the amplitude method. The allowed (95% C.L.) $\bar{\rho}$–$\bar{\eta}$ region is shown in Fig. 1. The triangle drawn is to facilitate our discussions, and corresponds to the central values of the fits, $(\alpha, \beta, \gamma) = (93^\circ, 24^\circ, 63^\circ)$.

The CP angles α, β and γ can be measured in CP-violating rate asymmetries in B decays. These angles can be expressed in terms of $\bar{\rho}$ and $\bar{\eta}$. Thus, different shapes of the unitarity triangle are equivalent to different values of the CP angles. Referring to Fig. 1, the allowed ranges at 95% C.L. are given by

$$75^\circ \leq \alpha \leq 121^\circ \ , \quad 16^\circ \leq \beta \leq 34^\circ \ , \quad 38^\circ \leq \gamma \leq 81^\circ \ , \tag{12}$$

or, equivalently,

$$-0.88 \leq \sin 2\alpha \leq 0.50 \ , \quad 0.53 \leq \sin 2\beta \leq 0.93 \ , \quad 0.38 \leq \sin^2\gamma \leq 0.98 \ . \tag{13}$$

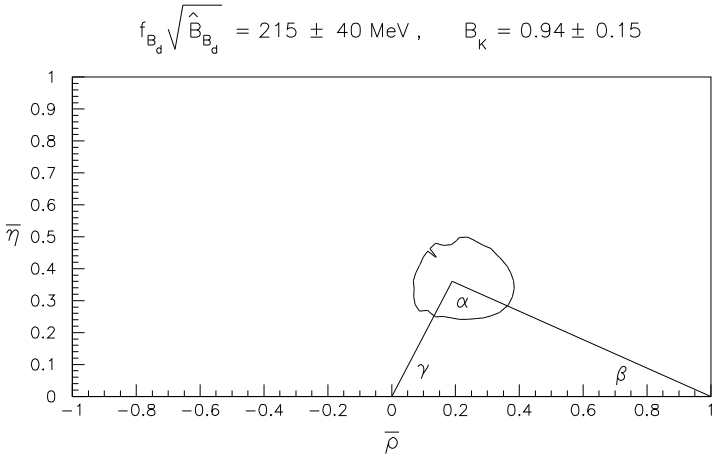

Figure 1: Allowed region in $\bar{\rho}$–$\bar{\eta}$ space in the SM, from a fit to the ten parameters discussed in the text and given in Table 1. The solid line represents the region with $\chi^2 = \chi^2_{min} + 6$ corresponding to the 95% C.L. region. The triangle shows the best fit.

Of course, the values of α, β and γ are correlated, i.e. they are not all allowed simultaneously. After all, the sum of these angles must equal 180°. We illustrate these correlations in Figs. 2 and 3. In both of these figures, the SM plot is labelled by $f = 0$. Fig. 2 shows the allowed region in $\sin 2\alpha$–$\sin 2\beta$ space allowed by the data. And Fig. 3 shows the allowed (correlated) values of the CP angles α and γ. This correlation is roughly linear, due to the relatively small allowed range of β [Eq. (12)].

The allowed ranges for the CKM-parameters obtained from our unitarity fits can be compared with those obtained by other groups. For example, concentrating on $\sin 2\alpha$ and $\sin 2\beta$, Plaszczynski and Schune get the following (95% C.L.) ranges [6]:

$$-0.95 \leq \sin 2\alpha \leq 0.50 \quad , \qquad 0.50 \leq \sin 2\beta \leq 0.85 \quad , \tag{14}$$

which are very similar to the ranges obtained by us for these quantities [Eq. (13)]. While there are smallish differences in the input parameters from experimental measurements, the real difference in the two fits lies in the incorporation of the theoretical uncertainties. We have treated theoretical and experimental errors on the same footing. On the other hand, Plaszczynski and Schune have

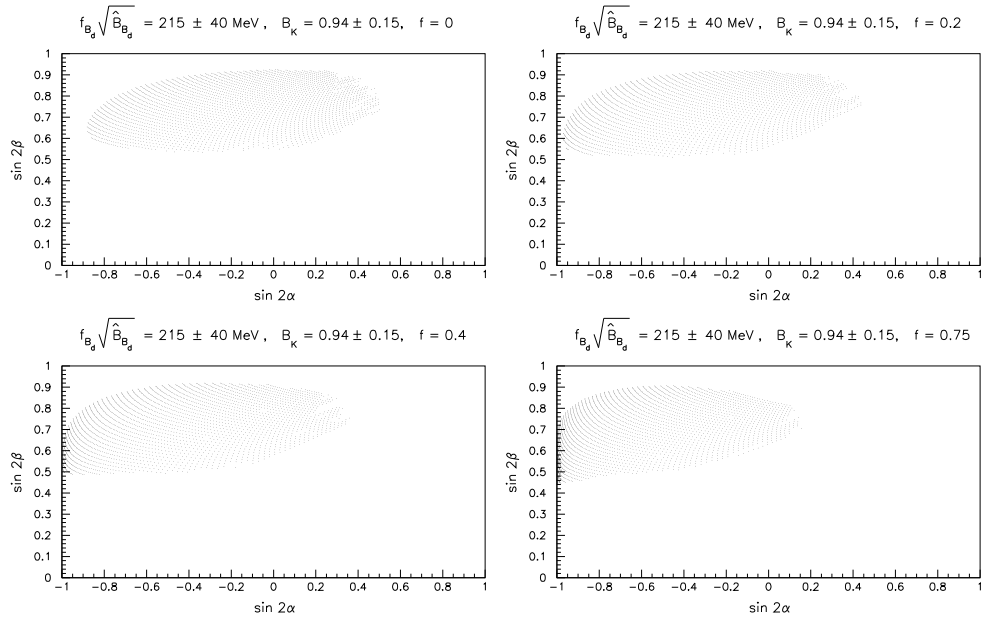

Figure 2: Allowed 95% C.L. region of the CP-violating quantities $\sin 2\alpha$ and $\sin 2\beta$, from a fit to the data given in Table 1. The upper left plot ($f = 0$) corresponds to the SM, while the other plots ($f = 0.2, 0.4, 0.75$) correspond to various SUSY models.

scanned over a "reasonable range" of theoretical parameters, determined the allowed contours for fixed values of these parameters and taken the envelope of all the individual contours obtained in the allowed range. Of course, the size of the resulting envelope depends on the assumed theoretical range, so that a certain amount of subjectivity is already embedded. Given that the parametric input in the present analysis and in [6] are similar, the closeness of the two fits implies that they do not depend sensitively on the prescription for handling theoretical errors.

In fact, one can turn the argument around: with improved limits on (or an actual measurement of) ΔM_s, the theoretical errors on $f_{B_d}\sqrt{\hat{B}_{B_d}}$ and $\hat{B}_K$ can be effectively reduced. To quantify these remarks, we examine the presently-allowed correlation in the parameters $\hat{B}_K$ and $f_{B_d}\sqrt{\hat{B}_{B_d}}$ which follows from our fits in the SM. Recall that the theoretically-allowed ranges for these quantities are $f_{B_d}\sqrt{\hat{B}_{B_d}} = 215 \pm 40$ MeV and $\hat{B}_K = 0.94 \pm 0.15$. Rather than present the 95% c.l. region in the $\bar{\rho}$–$\bar{\eta}$ plane (Fig. 1), we use the fits to find the allowed 95%

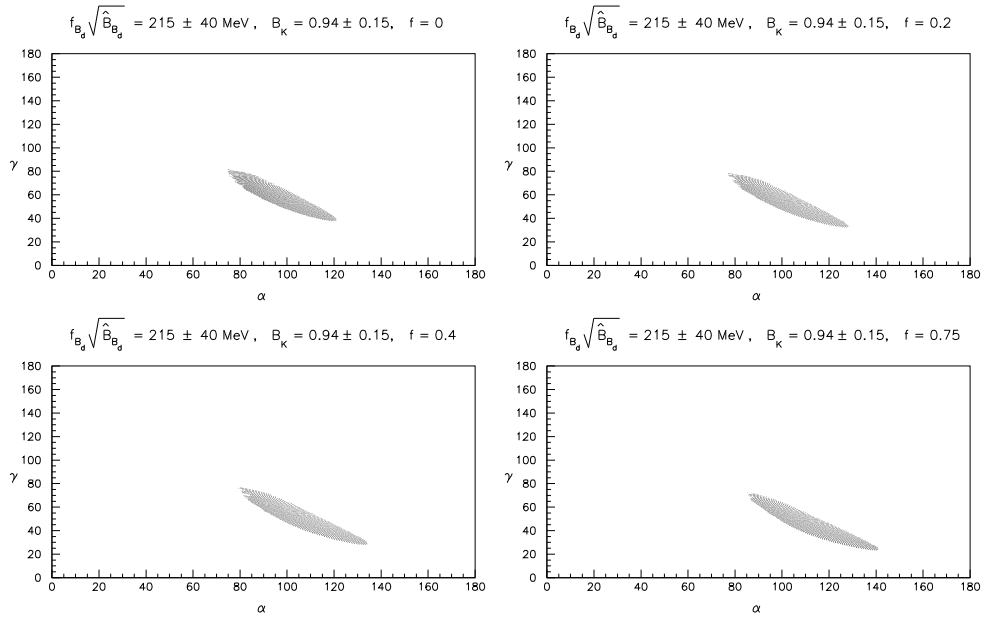

Figure 3: Allowed 95% C.L. region of the CP-violating quantities α and γ, from a fit to the data given in Table 1. The upper left plot ($f = 0$) corresponds to the SM, while the other plots ($f = 0.2,\ 0.4,\ 0.75$) correspond to various SUSY models.

c.l. region in the $\hat{B}_K$–$f_{B_d}\sqrt{\hat{B}_{B_d}}$ plane. The results are shown in Fig. 4, where we have allowed the hadronic parameters to vary in the range 135 MeV $\leq f_{B_d}\sqrt{\hat{B}_{B_d}} \leq 295$ MeV and $0.64 \leq \hat{B}_K \leq 1.24$, which corresponds to allowing a $\pm 2\sigma$ uncertainty on each. (Note that there appears to be some structure near the solid line on the left-hand side of the figure. This is a numerical artifact due to the binning of the ΔM_s data, and can be ignored. Only the solid line is important.) Only values of $f_{B_d}\sqrt{\hat{B}_{B_d}}$ and $\hat{B}_K$ which lie between the two solid lines in Fig. 4 are allowed at the 95% C.L. Note that present data do not allow a value $f_{B_d}\sqrt{\hat{B}_{B_d}} \leq 165$ MeV. Likewise, values of $f_{B_d}\sqrt{\hat{B}_{B_d}}$ in excess of 230 MeV are highly correlated with the value of $\hat{B}_K$. Thus, no values in excess of 230 MeV are allowed for $f_{B_d}\sqrt{B_{B_d}}$ if $\hat{B}_K \leq 0.6$ in the SM. This is very similar (though not identical) to the correlation shown in Ref. [6].

Of course, one obtains more stringent constraints on the CKM parameters if significantly reduced errors are assumed for the input parameters. For example, a recent fit [7], assuming $\delta V_{ub}/V_{cb} = \pm 8.8\%$ (compared to $\delta V_{ub}/V_{cb} =$

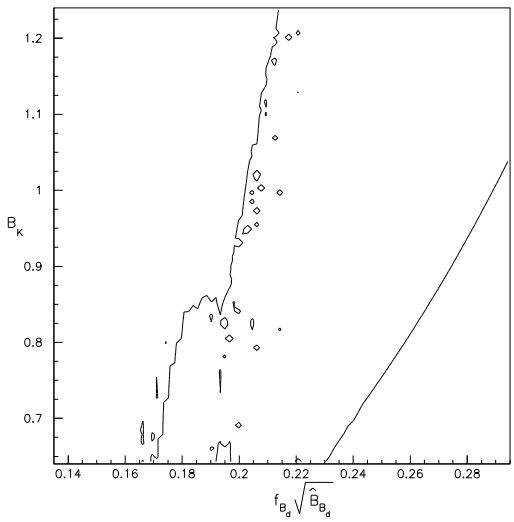

Figure 4: Allowed 95% C.L. region of the non-perturbative quantities $\hat{B}_K$ and $f_{B_d}\sqrt{\hat{B}_{B_d}}$ which results from the CKM fits in the SM.

$\pm 15\%$ used here), and $f_{B_d}\sqrt{\hat{B}_{B_d}} = 220 \pm 28$ MeV (as opposed to $f_{B_d}\sqrt{\hat{B}_{B_d}} = 215 \pm 40$ MeV in Table 1), leads to a more precise determination of the apex of the unitarity triangle. In turn, this yields the following 95% C.L. ranges for the CP asymmetries [7]:

$$-0.73 \leq \sin 2\alpha \leq 0.26 \ , \quad 0.63 \leq \sin 2\beta \leq 0.81 \ , \quad 0.51 \leq \sin^2 \gamma \leq 0.93 \ . \quad (15)$$

3 Unitarity Triangle: A SUSY Profile

In this section we update the profile of the unitarity triangle in supersymmetric (SUSY) theories. In general, minimal supersymmetric standard models (MSSM) have three physical phases, apart from the QCD vacuum parameter $\bar{\theta}_{QCD}$ which we shall take to be zero. The three phases are: (i) the CKM phase represented here by the Wolfenstein parameter η, (ii) the phase $\theta_A = \arg(A)$, and (iii) the phase $\theta_\mu = \arg(\mu)$ [27]. The last two phases, residing in the soft SUSY-breaking terms and in the scalar superpotential, are peculiar to SUSY models and their effects must be taken into account in a general supersymmetric framework. In particular, the CP-violating asymmetries which result from the

interference between mixing and decay amplitudes can produce non-standard effects. Concentrating here on the $\Delta B = 2$ amplitudes, two new phases θ_d and θ_s arise, which can be parametrized as follows [28]:

$$\theta_{d,s} = \frac{1}{2} \arg \left(\frac{\langle B_{d,s} | \mathcal{H}_{eff}^{SUSY} | \bar{B}_{d,s} \rangle}{\langle B_{d,s} | \mathcal{H}_{eff}^{SM} | \bar{B}_{d,s} \rangle} \right) \ , \tag{16}$$

where $\mathcal{H}^{SUSY}$ is the effective Hamiltonian including both the SM degrees of freedom and the SUSY contributions. Thus, CP-violating asymmetries in B decays would involve not only the phases α, β and γ, defined previously, but additionally θ_d or θ_s. In other words, the SUSY contributions to the real parts of $M_{12}(B_d)$ and $M_{12}(B_s)$ are *no longer proportional* to the CKM matrix elements $V_{td}V_{tb}^*$ and $V_{ts}V_{tb}^*$, respectively. If θ_d or θ_s were unconstrained, one could not make firm predictions about the CP asymmetries in SUSY models. In such a case, an analysis of the profile of the unitarity triangle in such models would be futile.

However, the experimental upper limits on the electric dipole moments (EDMs) of the neutron and electron [9] do provide a constraint on the phase θ_μ [29]. In supergravity (SUGRA) models with *a priori* complex parameters A and μ, the phase θ_μ is strongly bounded with $\theta_\mu < 0.01\pi$ [30].

As for the phase θ_A, it can be of $O(1)$ in the small θ_μ region, as far as the EDMs are concerned. However, in both the $\Delta S = 2$ and $\Delta B = 2$ transitions, and for low-to-moderate values of $\tan\upsilon$ [1], it has been shown that θ_A does not change the phase of either the matrix element $M_{12}(K)$ [27] or of $M_{12}(B)$ [30]. Hence, in SUGRA models, $\arg M_{12}(B)|_{SUGRA} = \arg M_{12}(B)|_{SM} = \arg(\xi_t^2)$, where $\xi_t = V_{td}^* V_{tb}$. Likewise, the phase of the SUSY contribution in $M_{12}(K)$ is aligned with the phase of the $t\bar{t}$-contribution in $M_{12}(K)$, given by $\arg(V_{td}V_{ts}^*)$.

Thus, in SUGRA models, one can effectively set $\theta_d \simeq 0$ and $\theta_s \simeq 0$, so that the CP-violating asymmetries give information about the SM phases α, β and γ. Hence, an analysis of the UT and CP-violating phases α, β and γ can

[1] In supersymmetric jargon, the quantity $\tan\beta$ is used to define the ratio of the two vacuum expectation values (vevs) $\tan\beta \equiv v_u/v_d$, where $v_d(v_u)$ is the vev of the Higgs field which couples exclusively to down-type (up-type) quarks and leptons. (See, for example, the review by Haber in Ref. [9]). However, in discussing flavour physics, the symbol β is traditionally reserved for one of the angles of the unitarity triangle. To avoid confusion, we will call the ratio of the vevs $\tan\upsilon$.

be carried out in a very similar fashion as in the SM, taking into account the additional contributions to $M_{12}(K)$ and $M_{12}(B)$.

3.1 NLO Corrections to ΔM_d, ΔM_s and ϵ in Minimal SUSY Flavour Violation

A number of SUSY models share the features mentioned in the previous subsection, and the supersymmetric contributions to the mass differences $M_{12}(B)$ and $M_{12}(K)$ have been analyzed in a number of papers [30, 31, 32, 33, 34], following the pioneering work of Ref. [35]. The SUSY contributions to ΔM_d, ΔM_s and $|\epsilon|$ in supersymmetric theories can be incorporated in a simple form [4]:

$$\begin{aligned}
\Delta M_d &= \Delta M_d(SM)[1 + f_d(m_{\chi_2^\pm}, m_{\tilde{t}_R}, m_{H^\pm}, \tan\upsilon)], \\
\Delta M_s &= \Delta M_s(SM)[1 + f_s(m_{\chi_2^\pm}, m_{\tilde{t}_R}, m_{H^\pm}, \tan\upsilon)], \\
|\epsilon| &= \frac{G_F^2 f_K^2 M_K M_W^2}{6\sqrt{2}\pi^2 \Delta M_K} \hat{B}_K \left(A^2\lambda^6\bar{\eta}\right) \left(y_c \left\{\hat{\eta}_{ct} f_3(y_c, y_t) - \hat{\eta}_{cc}\right\}\right. \\
&\quad \left. + \hat{\eta}_{tt} y_t f_2(y_t)[1 + f_\epsilon(m_{\chi_2^\pm}, m_{\tilde{t}_2}, m_{H^\pm}, \tan\upsilon)] A^2\lambda^4(1-\bar{\rho})\right). \quad (17)
\end{aligned}$$

The quantities f_d, f_s and f_ϵ can be expressed as

$$f_d = f_s = \frac{\hat{\eta}_{2,S}(B)}{\hat{\eta}_B} R_{\Delta_d}(S) \ , \qquad f_\epsilon = \frac{\hat{\eta}_{2,S}(K)}{\hat{\eta}_{tt}} R_{\Delta_d}(S) \ , \qquad (18)$$

where $R_{\Delta_d}(S)$ is defined as

$$R_{\Delta_d}(S) \equiv \frac{\Delta M_d(SUSY)}{\Delta M_d(SM)}(LO) = \frac{S}{y_t f_2(y_t)} \ . \qquad (19)$$

The supersymmetric function S is given in Ref. [35], and the NLO functions $\hat{\eta}_{2,S}(B)$ and $\hat{\eta}_{2,S}(K)$ can be found in Ref. [36]. The functions f_i, $i = d, s, \epsilon$ are all positive definite, i.e. the supersymmetric contributions add *constructively* to the SM contributions in the entire allowed supersymmetric parameter space. The two QCD correction factors appearing in Eq. (18) are numerically very close to one another, with $\hat{\eta}_{2,S}(B)/\hat{\eta}_B \simeq \hat{\eta}_{2,S}(K)/\hat{\eta}_{tt} = 0.93$ [4]. Thus, to an excellent approximation, one has $f_d = f_s = f_\epsilon \equiv f$.

How big can f be? This quantity is a function of the masses of the top squark, chargino and the charged Higgs, $m_{\tilde{t}_R}$, $m_{\tilde{\chi}_2^\pm}$ and $m_{H^\pm}$, respectively, as well as of $\tan\upsilon$. The maximum allowed value of f depends on the model (minimal SUGRA, non-minimal SUGRA, MSSM with constraints from EDMs, etc.). From the published results we conclude that typically f can be as large

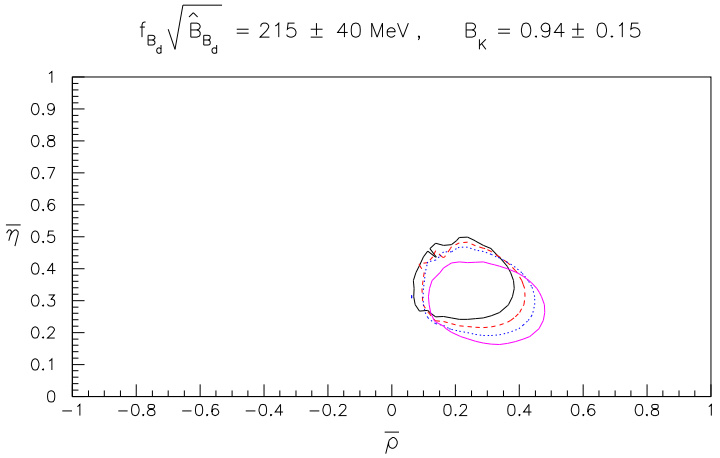

Figure 5: Allowed 95% C.L. region in ρ–η space in the SM and in SUSY models, from a fit to the data given in Table 1. From left to right, the allowed regions correspond to $f = 0$ (SM, solid line), $f = 0.2$ (long dashed line), $f = 0.4$ (short dashed line), $f = 0.75$ (dotted line).

as 0.45 in non-minimal SUGRA models for low $\tan\upsilon$ (typically $\tan\upsilon = 2$) [34], and approximately half of this value in minimal SUGRA models [30, 33, 34]. Relaxing the SUGRA mass constraints, admitting complex values of A and μ but incorporating the EDM constraints, and imposing the constraints mentioned above, f could be larger [37]. In all cases, the value of f decreases with increasing $\tan\upsilon$ or increasing $m_{\tilde{\chi}_2^\pm}$ and $m_{\tilde{t}_R}$, as noted above.

3.2 SUSY Fits

For the SUSY fits, we use the same program as for the SM fits, except that the theoretical expressions for ΔM_d, ΔM_s and $|\epsilon|$ are modified as in Eq. (17). We compare the fits for four representative values of the SUSY function f — 0, 0.2, 0.4 and 0.75 — which are typical of the SM, minimal SUGRA models, non-minimal SUGRA models, and non-SUGRA models with EDM constraints, respectively.

The allowed 95% C.L. regions for these four values of f are all plotted in Fig. 5. As is clear from this figure, there is still a considerable overlap between the $f = 0$ (SM) and $f = 0.75$ regions. However, there are also regions allowed

Table 2: Allowed 95% C.L. ranges for the CP phases α, β and γ, as well as their central values, from the CKM fits in the SM ($f = 0$) and supersymmetric theories, characterized by the parameter f defined in the text.

f	α	β	γ	$(\alpha, \beta, \gamma)_{\rm cent}$
$f = 0$ (SM)	75° – 121°	16° – 34°	38° – 81°	$(93°, 24°, 63°)$
$f = 0.2$	77° – 128°	15° – 33°	32° – 78°	$(102°, 24°, 54°)$
$f = 0.4$	79° – 134°	15° – 33°	28° – 77°	$(108°, 23°, 49°)$
$f = 0.75$	86° – 141°	13° – 33°	23° – 72°	$(120°, 21°, 39°)$

for one value of f which are excluded for another value. Thus a sufficiently precise determination of the unitarity triangle might be able to exclude certain values of f (including the SM, $f = 0$).

From Fig. 5 it is clear that a measurement of the CP angle β will *not* distinguish among the various values of f. Rather, it is the measurement of γ or α which has the potential to rule out certain values of f. As f increases, the allowed region moves slightly down and towards the right in the $\bar{\rho}$–$\bar{\eta}$ plane, corresponding to smaller values of γ (or equivalently, larger values of α). We illustrate this in Table 2, where we present the allowed ranges of α, β and γ, as well as their central values (corresponding to the preferred values of $\bar{\rho}$ and $\bar{\eta}$), for each of the four values of f. From this Table, we see that the allowed range of β is largely insensitive to the model. Conversely, the allowed values of α and γ do depend somewhat strongly on the chosen value of f. Note, however, that one is not guaranteed to be able to distinguish among the various models: as mentioned above, there is still significant overlap among all four models. Thus, depending on what values of α and γ are obtained, we may or may not be able to rule out certain values of f.

For completeness, in Table 3 we present the corresponding allowed ranges for the CP asymmetries $\sin 2\alpha$, $\sin 2\beta$ and $\sin^2 \gamma$. Again, we see that the allowed range of $\sin 2\beta$ is largely independent of the value of f. On the other hand, as f increases, the allowed values of $\sin 2\alpha$ become increasingly negative, while those of $\sin^2 \gamma$ become smaller.

The allowed (correlated) values of the CP angles for various values of f can be clearly seen in Figs. 2 and 3. As f increases from 0 (SM) to 0.75, the change in the allowed $\sin 2\alpha$–$\sin 2\beta$ (Fig. 2) and α–γ (Fig. 3) regions is quite

Table 3: Allowed 95% C.L. ranges for the CP asymmetries $\sin 2\alpha$, $\sin 2\beta$ and $\sin^2\gamma$, from the CKM fits in the SM ($f = 0$) and supersymmetric theories, characterized by the parameter f defined in the text.

f	$\sin 2\alpha$	$\sin 2\beta$	$\sin^2\gamma$
$f = 0$ (SM)	-0.88 – 0.50	0.53 – 0.93	0.38 – 0.98
$f = 0.2$	-0.97 – 0.44	0.51 – 0.92	0.29 – 0.96
$f = 0.4$	-1.00 – 0.36	0.49 – 0.92	0.22 – 0.95
$f = 0.75$	-1.00 – 0.16	0.44 – 0.91	0.16 – 0.91

significant.

4 Conclusions

In the very near future, CP-violating asymmetries in B decays will be measured at B-factories, HERA-B and hadron colliders. Such measurements will give us crucial information about the interior angles α, β and γ of the unitarity triangle. If we are lucky, there will be an inconsistency in the independent measurements of the sides and angles of this triangle, thereby revealing the presence of new physics.

An interesting possibility, from the point of view of making predictions, are models which contribute to B^0–$\overline{B^0}$ mixings and $|\epsilon|$, but without new phases. One type of new physics which does just this is supersymmetry (SUSY). There are some SUSY models which do contain new phases, but they suffer from a lack of predictivity. However, there is also a large class of SUSY models with no new phases. In these models, there are new, supersymmetric contributions to K^0–$\overline{K^0}$, B^0_d–$\overline{B^0_d}$ and B^0_s–$\overline{B^0_s}$ mixing. The key ingredient in our analysis is the fact that these contributions, which add constructively to the SM, depend on the SUSY parameters in essentially the same way. That is, so far as an analysis of the unitarity triangle is concerned, there is a single parameter, f, which characterizes the various SUSY models within this class of models ($f = 0$ corresponds to the SM).

We have therefore updated the profile of the unitarity triangle in both the SM and some variants of the MSSM. We have used the latest experimental data on $|V_{cb}|$, $|V_{ub}/V_{cb}|$, ΔM_d and ΔM_s, as well as the latest theoretical estimates (including errors) of $\hat{B}_K$, $f_{B_d}\sqrt{\hat{B}_{B_d}}$ and $\xi_s \equiv f_{B_d}\sqrt{\hat{B}_{B_d}}/f_{B_s}\sqrt{\hat{B}_{B_s}}$. In addition

to $f = 0$ (SM), we considered three SUSY values of f: 0.2, 0.4 and 0.75, representing the minimal SUGRA models, non-minimal SUGRA models, and non-SUGRA models with EDM constraints, respectively.

We first considered the profile of the unitarity triangle in the SM, shown in Fig. 1. We then compared the SM with the different SUSY models. The result can be seen in Fig. 5. As f increases, the allowed region moves slightly down and to the right in the $\bar{\rho}$–$\bar{\eta}$ plane. The main conclusion from this analysis is that the measurement of the CP angle β will not distinguish among the SM and the various SUSY models – the allowed region of β is virtually the same in all these models. On the other hand, the allowed ranges of α and γ do depend on the choice of f. For example, larger values of f tend to favour smaller values of γ. The dependence of the CP angles on the value of f is illustrated clearly in Tables 2 and 3. Thus, with measurements of γ or α, we may be able to rule out certain values of f (including the SM, $f = 0$). However, we also note that there is no guarantee of this happening – at present there is still a significant region of overlap among all four models.

Acknowledgements:

One of us (A.A.) would like to thank the organizers of the DAPHNE '99 workshop, in particular Giorgio Capon and Gino Isidori, for their kind hospitality. The work of D.L. was financially supported by NSERC of Canada.

References

1. N. Cabibbo, Phys. Rev. Lett. **10**, 531 (1963); M. Kobayashi and K. Maskawa, Prog. Theor. Phys. **49**, 652 (1973).

2. L. Wolfenstein, Phys. Rev. Lett. **51**, 1945 (1983).

3. A.J. Buras, M.E. Lautenbacher and G. Ostermaier, Phys. Rev. **D50**, 3433 (1994).

4. A. Ali and D. London, Eur. Phys. J. **C9**, 687 (1999); Phys. Rep. **320**, 79 (1999).

5. G. Blaylock, Plenary talk, XIX International Symposium on Lepton and Photon Interactions at High Energies, Stanford, August 9 - 14,

1999. For details, see the LEP B-Oscillations Working Group webcite, http://www.cern.ch/LEPBOSC/.

6. S. Plaszczynski and M.-H. Schune, Report LAL 99-67 (hep-ph/9911280).
7. M. Bargiotti et al., Report HERA-B 00-012 (2000).
8. M. Ciuchini, G. Degrassi, P. Gambino and G.F. Giudice, Nucl. Phys. **B534**, 3 (1998).
9. C. Caso et al. (Particle Data Group), Eur. Phys. J. **C3**,1 (1998).
10. F. Parodi, in *Proc.* of XXIXth. Int. Conf. on High Energy Physics, Vancouver, B.C., 1998.
11. A.J. Buras, W. Slominski, and H. Steger, Nucl. Phys. **B238**, 529 (1984); *ibid.* **B245**,369 (1984).
12. T. Inami and C.S. Lim, Progr. Theor. Phys. **65**, 297 (1981).
13. S. Herrlich and U. Nierste, Nucl. Phys. **B419**, 292 (1994).
14. A.J. Buras, M. Jamin and P.H. Weisz, Nucl. Phys. **B347**, 491 (1990).
15. S. Herrlich and U. Nierste, Phys. Rev. **D52**, 6505 (1995).
16. T. Draper, preprint hep-lat/9810065 (1998); S. Sharpe, preprint hep-lat/9811006 (1998).
17. C. Bernard et al., Phys. Rev. Lett. **81**, 4812 (1998).
18. H.G. Moser and A.. Roussarie, Nucl. Instr. Meth. **A384**, 491 (1997).
19. A. Alavi-Harati et al. (KTEV), Phys. Rev. Lett. **83**, 22 (1999).
20. V. Fanti et al. (NA48), Phys. Lett. **B465**, 335 (1999).
21. G.D. Barr et al. (NA31), Phys. Lett. **B317** (1993) 233.
22. L.K. Gibbons et al. (E731), Phys. Rev. Lett. **70**, 1203 (1993).
23. L. Wolfenstein, Phys. Rev. Lett. **13**, 380 (1964).

24. A.J. Buras, M. Jamin and M.E. Lautenbacher, Nucl. Phys. **B370**, 69 (1992); *ibid.* **B400**, 37 (1993); *ibid.* **B400**, 75 (1993); *ibid.* **B408**, 209 (1993); M. Ciuchini et al., Phys. Lett. **B301**, 263 (1993); Nucl. Phys. **B415**, 403 (1994); S. Bertolini, M. Fabbrichesi and J.O. Egg, Nucl. Phys. **B499**, 197 (1995); *ibid.* **B476**,225 (1996).

25. A.J. Buras and L. Silvestrini, Nucl. Phys. **B546**, 299 (1999); S. Bosch et al., preprint hep-ph/9904408; Y. Keum, U. Nierste, A. Sanda, Phys. Lett. **B457**, 157 (1999); T. Hambye et al., preprint hep-ph/9906434; G. Martinelli (these proceedings).

26. C.A. Blocker (CDF), these proceedings.

27. M. Dugan, B. Grinstein and L.J. Hall, Nucl. Phys. **B255**, 413 (1985); S. Dimopoulos and S. Thomas, Nucl. Phys. **B465**, 23 (1996).

28. A.G. Cohen, D.B. Kaplan and A.E. Nelson, Phys. Lett. **B388**, 588 (1996); A.G. Cohen, D.B. Kaplan, F. Lepeintre and A.E. Nelson, Phys. Rev. Lett. **78**, 2300 (1997).

29. T. Falk, K.A. Olive and M. Srednicki, Phys. Lett. **B354**, 99 (1995); T. Falk and K.A. Olive, *ibid.* **B375**, 196 (1996).

30. T. Nihei, Prog. Theor. Phys. **98**, 1157 (1997).

31. G.C. Branco, G.C. Cho, Y. Kizukuri and N. Oshimo, Phys. Lett. **B337**, 316 (1994); Nucl. Phys. **B449**, 483 (1995).

32. T. Goto, T. Nihei and Y. Okada, Phys. Rev. **D53** (1996) 5233.

33. T. Goto et al., Phys. Rev. **D55** (1997) 4273.

34. T. Goto, Y. Okada and Y. Shimizu, Phys. Rev. **D58**: 094006 (1998); preprint KEK-TH-611, hep-ph/9908499.

35. S. Bertolini, F. Borzumati, A. Masiero and G. Ridolphi, Nucl. Phys. **B353**, 591 (1991).

36. F. Krauss and G. Soff, preprint hep-ph/9807238.

37. S. Baek and P. Ko, Phys. Rev. Lett. **83**, 488 (1999).